Biochimica et Biophysica Acta, 368 (1974) 181–198

BBA 46823

STATE OF CHLOROPHYLL *a* IN VITRO AND IN VIVO FROM ELECTRONIC TRANSITION SPECTRA, AND THE NATURE OF ANTENNA CHLOROPHYLL*

T. M. COTTON, A. D. TRIFUNAC, K. BALLSCHMITER** and J. J. KATZ

Chemistry Division, Argonne National Laboratory, Argonne, Ill. 60439 (U.S.A.)

(Received June 14th, 1974)

SUMMARY

The computer deconvolution of the red envelopes of visible spectra of chlorophyll *a* solutions in dry nonpolar solvents is described. In solvents such as carbon tetrachloride and benzene chlorophyll *a* is present in dimer form in the concentration range of 10^{-6}–10^{-2}. In solvents such as hexane and *n*-alkanes oligomeric species of chlorophyll *a* are present. The relative intensities of the Gaussian components used in the spectral deconvolution can be related to the size and conformation of the chlorophyll *a* aggregates. While the computer deconvolution is basically a heuristic method, it is suggested that it is based on a sound physical rationale. A comparison of the computer deconvoluted visible spectra of photosynthetic organisms with those of solutions of chlorophyll *a* oligomers in nonpolar media provides good evidence that antenna chlorophyll in green plants has spectral properties that are very similar, if not identical, to those of chlorophyll *a* oligomers, $(\text{chlorophyll}_2)_n$.

INTRODUCTION

Absorption spectroscopy in the visible (also referred to here as electronic transition spectroscopy) has been the most widely used experimental technique for the study of the light conversion act in photosynthesis. In all photosynthetic organisms, the main long wavelength absorption band in the red is due to chlorophyll *a* (plants) or bacteriochlorophyll (photosynthetic bacteria). Close examination of this region of the spectrum has resulted in the widely accepted view that only a small fraction of the chlorophyll *a* in green plants is photo-active, and that the bulk of the chlorophyll *a* in green plants serves in an accessory capacity as a light gatherer [1]. This accessory or antenna chlorophyll *a* absorbs maximally near 680 nm. We have considered the nature of photosynthetic reaction center chlorophyll elsewhere [2–5]. Here we will be concerned entirely with the spectral properties of in vitro analogs of antenna chlorophyll *a* in green plants.

* Work performed under the auspices of the U.S. Atomic Energy Commission.
** Resident Research Associate, 1967-1969.

Investigations on the electron transition spectrum of chlorophyll *a* in defined media [6–11] establish that chlorophyll *a* in electron donor (polar, basic, nucleophilic) solvents such as methanol, acetone, tetrahydrofuran, pyridine and the like shows a single major red maximum lying between 661 and 670 nm, with the exact position and band half width dependent on the dielectric constant and refractive index of the solvent [8]. In dry benzene and carbon tetrachloride, the red band of chlorophyll *a* in dilute solution developes a distinct shoulder near 680 nm on the long wavelength side of the principal band [12–15]. The intensity of absorption at the red shoulder is concentration dependent, especially in hydrocarbon solvents [16].

Most of the data on electronic transition spectra of chlorophyll *a* are based on dilute solutions. In the plant, the chlorophyll *a* is to the contrary highly concentrated. Rabinowitch [17] estimates that the chlorophyll concentration of chloroplasts may be as great as 0.2 M. We are convinced that the widely-held opinion that there are major differences between the in vivo and in vitro chlorophyll *a* electronic transmission spectra arises primarily from the fact that the in vivo spectra are recorded on concentrated chlorophyll *a* systems, whereas the laboratory data are almost always recorded on dilute solutions in which the clorophyll *a* has generally been disaggregated by water or some other adventitious nucleophile. One of the principal objects of the present communication is to show that in vitro spectra recorded on highly concentrated chlorophyll *a* solutions in dry nonpolar solvents are much more pertinent and useful to the interpretation of in vivo spectra. Such a conclusion is, in fact, implicit in the older literature. Thus, it has been known for a long time that long wavelength forms of chlorophyll *a* can be generated in the form of films or colloidal dispersions that closely mimic the long wavelength forms of chlorophyll *a* in the plant [18–20] (Ballschmiter, K., Cotton, T. M. and Katz, J. J., unpublished). Films, to be sure, are essentially highly concentrated chlorophyll solutions [21]. As indicated in the next section, long wavelength forms of chlorophyll *a* in vitro arise either from chlorophyll *a*-chlorophyll *a* self-interactions or from chlorophyll *a*-bifunctional ligand interactions. In both instances, long wavelength forms are associated with chlorophyll *a* at relatively high concentrations, say greater than $5 \cdot 10^{-3}$M.

Investigations by infrared [22–27] and nuclear magnetic resonance [28–31] spectroscopy have revealed that chlorophyll *a* is a molecule with an unusual combination of electron donor and acceptor properties. These studies strongly suggest that the central magnesium atom of chlorophyll *a* with coordination number 4 is coordinatively unsaturated to such an extent that at least one of the magnesium axial positions must be occupied by an electron donor group [32]. In the absence of any other nucleophiles, as in nonpolar solvents, another chlorophyll *a* molecule can act as electron donor via the keto carbonyl oxygen function of Ring V. Recent ^{13}C nuclear magnetic resonance experiments [33] on chlorophyll *a* give strong supporting evidence for the involvement of the keto C=O function of Ring V as electron donor to magnesium. The coordination interaction between chlorophyll *a* molecules acting as acceptor at magnesium and donor at keto C=O forms chlorophyll *a* dimers and higher oligomers whose existence has been confirmed by molecular weight measurements by vapor phase osmometry [34] and by ultracentrifugation studies (to be published). When the electron donor is monofunctional (acetone, tetrahydrofuran, triethylamine, pyridine, etc.) species of the general type, chlorophyll $\cdot L_1$ and chlorophyll $\cdot L_2$ are formed. Bifunctional nucleophiles, such as dioxane, pyrazine,

4,4′-bipyridine, and 1,4′-diazabicyclo(2.2.2)octane, form chlorophyll *a* adducts in aliphatic hydrocarbon solvent media in which chlorophyll *a* molecules are cross-linked through magnesium atoms to form aggregates (micelles) of high molecular weight [35] (Cotton, T. M., Ballschmiter, K. and Katz, J. J., unpublished). Whether a ligand is mono- or bi-functional depends on both the chlorophyll *a* and the ligand concentration, and the nonpolar solvent itself. Thus, water is a monofunctional ligand in benzene and carbon tetrachloride, but acts as a bifunctional ligand in chlorophyll *a* solutions ($> 10^{-3}$M) in aliphatic hydrocarbon solvents [36].

Laboratory data establishes that all chlorophyll species of the type, chlorophyll · L_1 and chlorophyll · L_2, where L is an electron donor ligand, are short wavelength forms absorbing light at wavelengths lower than 671 nm (in pyridine), and mostly in the range 661–665 nm [8]. Chlorophyll *a* adducts with bifunctional ligands are all red-shifted species, very often considerably so. The (chlorophyll · $H_2O)_n$ adduct, to cite the most remarkable instance, absorbs maximally at 743 nm, a red shift of no less than 80 nm [36]. The chlorophyll–chlorophyll endogamous species, the dimer (chlorophyll$_2$), and the oligomer (chlorophyll$_2)_n$, however, are only moderately red-shifted. It is important to realize that the self-aggregation of chlorophyll *a* yields chlorophyll *a* species in which the geometry of the chlorophyll *a* molecules relative to each other is such as to give rise to only small red shifts.

In this paper, our chief concern will be with the electronic transition spectra of chlorophyll *a* dimer and oligomer. We have recorded spectra of these species over a large concentration range (10^{-6}–10^{-1} M) with scrupulous attention to the exclusion of water, adventitious nucleophiles, and air. We have applied extensive computer deconvolution techniques, to our knowledge for the first time, to the in vitro data*.

C. S. French and co-workers [37–45] and others [46–48] have examined and deconvoluted a large number of spectra of in vivo systems at liquid N_2 temperature. Because low temperature spectra exhibit more fine structure, a large number of Gaussian/Lorenztian components were used in the deconvolution. At present, we feel that a computer deconvolution study of the in vivo chlorophyll *a* spectrum requires, as a necessary preliminary, a study of the more easily defined in vitro systems, in order to be able to correlate spectra with defined chlorophyll *a* species.

We are primarily interested in this paper in the spectral properties of in vitro chlorophyll *a* species. We have therefore applied the methods and procedures described here to the visible spectra of antenna or bulk chlorophyll *a* in the plant, and at the end of this paper give results that support the hypothesis that antenna or bulk chlorophyll *a* in the plant has spectral properties and structure very similar to chlorophyll *a* oligomers, (chlorophyll$_2)_n$, characteristically present in concentrated solutions of chlorophyll *a* in aliphatic hydrocarbon solvents.

EXPERIMENTAL

Materials

Chlorophyll *a* was prepared by the method of Strain and Svec [49]. All hydrocarbon solvents used were the best grade available from Chemical Samples Co.

* The bacteriochlorophyll spectrum in carbon tetrachloride was deconvoluted by Sauer et al. [9]. However, their solutions contained some water thus raising some serious questions about the interpretation of their data.

(Columbus, Ohio). Hexadecane was washed with concentrated H_2SO_4, washed with $NaHCO_3$ solution and water, and then dried. Hydrocarbon solvents were dried over powered calcium hydride and Linde 3A molecular sieves. Methanol and carbon tetrachloride were dried over silica gel and stored over molecular sieves. All solvents were degassed on a vacuum line prior to use.

Solution preparation

All preparations were carried out in a N_2-purged dry box. All glassware, including absorption cells and syringes, were cleaned with CCl_4 and dried for at least 12 h in a vacuum oven at 80 °C before use and transferred from oven to dry box in a dessicator while still warm. Chlorophyll *a* was dried by the procedure of Ballschmiter et al. [50].

Instrumentation

Visible absorption spectra were recorded on a Cary 14 spectrophotometer equipped with a Datex SDS-1 digitizer. Spectra were measured in quartz cells with pathlengths from about 1 μm to 100 mm to accommodate chlorophyll *a* concentrations from 10^{-1} to 10^{-6} M. The sample chamber of the Cary was continuously purged with dry N_2 to maintain anhydrous conditions. The punched tapes produced by the digitizer were converted to punched cards on an IBM 1620 computer and the curve resolution computations were performed on the Applied Mathematics Division of ANL IBM 360/90 computer.

Digital computer deconvolution

A program written by the Applied Mathematics Division [51] at Argonne was used for curve resolution. The program utilizes the variable metric minimization procedure of Davidon [52] and fits component peaks by a least square fit to a Gaussian*:

$$y = \sum_{j=1}^{M} a_j e^{\frac{1}{2}(x-b_j)/c_j}$$

where a_j = peak height, b_j = peak location (nm), and c_j = standard deviation, or band half width (δ). As input, the number of desired peaks (M) and initial estimates for the parameters a_j, b_j, and c_j are specified. By successive iterations, the best fit is obtained. The outstanding feature of Davidon's method is that convergence is obtained even in most difficult non-linear situations. A minimization ε can be chosen to bring the fit as close as desired. In the work reported here, ε was chosen to be 10^{-9}.

The computer program allows the choice of Gaussian, Lorentzian, product of Gaussian and Lorentzian, and modified Gaussian-Lorentzian lineshapes. We have elected to use Gaussian lineshapes for the deconvolution components. For monomeric chlorophyll *a* species, the lineshape is observed to be very nearly Gaussian. Chlorophyll *a* solutions in pyridine over a range of concentrations, and chlorophyll *a* in *n*-hexane solutions to which pyridine, methanol, or tetrahydrofuran was added in a mole ratio of 10 : 1 gave spectra that were fitted very well by a single Gaussian at 663–665 nm with a half band width δ of 7–10 nm. In all these solutions, the chlorophyll *a* occurs largely as chlorophyll · L_1, where L is a molecule of solvent. The

* Other lineshape functions can also be used.

Gaussian lineshape for monomer chlorophyll *a* agrees with the observations of Cederstrand et al. [46]. In our opinion, the choice of Gaussian lineshape for the deconvolution, while somewhat arbitrary, has a better experimental basis and is more physically reasonable from statistical considerations of the behavior of large aggregates [53].

Consequently, we make the assumption that changes in the structure of the chlorophyll *a* species that occur in going from the most dilute to the most concentrated chlorophyll *a* solutions are gradual and progressive. In effect, a small change in concentration is assumed to result in a small change in the spectrum, and therefore a small change in the deconvolution. The deconvolution is thus required to be self-consistent over the entire concentration range. All the deconvolutions described here are made on the basis of this assumption, and the deconvolution for a given solvent system over the entire concentration range are, in fact, self-consistent.

All the data given in this paper has been replicated in completely independent experiments and in all cases reproducibility in replicate experiments was excellent. The estimated error in duplicate solutions for λ_3 and λ_4, the peak positions in nm, is $\pm$ 0.2 nm, while that for δ_3 and δ_4, the band half width in nm, is $\pm$ 0.2 nm. Gaussian component near 700 nm, which is always inserted to fit the red tail, is not necessarily to be identified with photoactive P700.

RESULTS AND DISCUSSION

Deconvolution of chlorophyll a spectra in polar solvents

Chlorophyll *a* dissolved in polar solvents (L) forms the monomeric species, chlorophyll · L_1 and chlorophyll · L_2 by coordination of the electron donor solvent to the central magnesium atom of the chlorophyll. The relative concentrations of the mono- and di-solvates present in particular systems is largely unknown. The presumption is that the magnesium favors the coordination number 5 (the mono-solvate) except under forcing conditions, as in a neat polar solvent, where hexa-coordinate magnesium (the di-solvate) would be formed by mass action. Even in a neat solvent, however, complete conversion to the hexa-coordinate state has not been established [54]. Chlorophyll *a* solutions in rigorously dried methanol, pyridine, and tetrahydrofuran were resolved into the components listed in Table I. The area of the major red absorption band relative to the total absorption between 600 and 720 nm was 62 % in all three solvents. However, pyridine and tetrahydrofuran were fitted with additional components at 640 and 630 nm, respectively. A band at 638 nm previously reported for pyridine [55] is absent when water is present. This apparent splitting of the minor absorption band in monomeric chlorophyll *a* is also observed in concentrated solutions of chlorophyll *a* in nonpolar solvents when tetrahydrofuran sufficient to disaggregate the chlorophyll *a* is present (100–1000 M tetrahydrofuran: 1 M chlorophyll *a*). Table I shows that there is only one minor band at 616 nm in dilute solution of chlorophyll · tetrahydrofuran in dodecane. At 10^{-1}M, however, an additional band is observed at 627 nm. For our present purposes, satisfactory fits for most of the envelope by a component with a Gaussian lineshape is of primary interest. Even the apparently simple monomer chlorophyll *a* systems are complex, and additional work will be needed for a more adequate interpretation of the spectra of these systems.

TABLE I

GAUSSIAN COMPONENTS OF THE DECONVOLUTED RED ENVELOPE OF MONOMER CHLOROPHYLL *a* IN VARIOUS SOLVENT SYSTEMS

Solvent	Concn (M)	λ_1 (nm)	δ_1 (nm)	% total area	λ_2 (nm)	δ_2 (nm)	% total area	λ_3 (nm)	δ_3 (nm)	% total area	λ_4 (nm)	δ_4 (nm)	% total area
Methanol	$1 \cdot 10^{-4}$	618	20	31				650	11	7	665.0	9.7	62
Pyridine	$6 \cdot 10^{-5}$	618	13	17	640	8	10	659	9	12	671.7	8.0	62
Tetrahydrofuran	$7 \cdot 10^{-5}$	613	13	16	630	8	8	654	9	15	665.0	7.1	62
Dodecane+methanol	$7 \cdot 10^{-5}$	616	13	19				650	10.8	13	663.0	6.7	68
Dodecane+tetrahydrofuran	$7 \cdot 10^{-7}$	616	15	19				650	10	11	661.7	6.3	70
Dodecane+tetrahydrofuran	$6 \cdot 10^{-2}$	607	15	10	627	14	17	650	6	4	663.1	7.6	70
Hexane+tetrahydrofuran	$6 \cdot 10^{-7}$	614	14	20				646	10	12	659.7	6.3	68
Hexane+tetrahydrofuran	$7.3 \cdot 10^{-2}$	611	10	10	626	10	8	646	10	8	661.4	6.9	74
Benzene+tetrahydrofuran	$9 \cdot 10^{-7}$	612	14	9	626	14	13	650	8	7	665.1	7.4	71
Benzene+tetrahydrofuran	$7 \cdot 10^{-2}$	611	14	12	631	14	13	652	8	5	665.4	7.3	70

TABLE II

GAUSSIAN COMPONENTS OF THE DECONVOLUTED RED ENVELOPE OF CHLOROPHYLL *a* IN CARBON TETRACHLORIDE AND BENZENE

Concn (M)	λ_1 (nm)	δ_1 (nm)	% total area	λ_2 (nm)	δ_2 (nm)	% total area	λ_3 (nm)	δ_3 (nm)	% total area	λ_4 (nm)	δ_4 (nm)	% total area	λ_5 (nm)	δ_5 (nm)	% total area
Carbon tetrachloride															
$1.2 \cdot 10^{-6}$	626	19	30	650	10	4	668.1	8.4	43	682.8	6.4	20	695	6.4	3
$1.0 \cdot 10^{-5}$	626	19	30	650	10	5	668.3	8.4	41	682.6	6.5	21	695	6.5	3
$1.2 \cdot 10^{-4}$	626	19	30	650	10	6	668.7	8.7	42	683.0	6.3	19	695	6.3	3
$1.2 \cdot 10^{-2}$	626	19	30	650	10	5	668.0	8.3	39	682.0	6.9	23	695	6.9	3
$9.1 \cdot 10^{-2}$	626	19	30	650	10	5	667.1	7.9	32	681.1	7.7	29	695	7.7	4
$1.2 \cdot 10^{-1}$	626	19	34	650	10	6	667.0	8.3	29	682.6	8.2	28	700	8.2	3
Benzene															
$1.4 \cdot 10^{-6}$	626	20	32	649	8	3	667.2	8.5	41	682.4	7.2	21	697	7.2	2
$1.4 \cdot 10^{-5}$	626	20	33	649	8	3	667.0	8.2	38	681.3	7.3	24	695	7.3	3
$1.4 \cdot 10^{-4}$	626	20	34	649	8	3	667.3	8.5	40	682.3	7.0	21	695	7.0	3
$2.7 \cdot 10^{-3}$	626	20	34	650	8	3	666.5	8.3	36	682.1	7.9	26	700	7.9	2
$2.6 \cdot 10^{-2}$	626	20	33	650	8	4	667.0	8.3	35	682.3	7.8	26	700	7.8	2
$1.3 \cdot 10^{-1}$	626	20	35	650	8	4	665.5	8.3	27	681.5	9.1	32	700	9.1	2

Deconvolution of dimer spectra

Molecular weight determinations by vapor phase osmometry [34] supported by infrared and nuclear magnetic resonance spectroscopy establish that chlorophyll *a* in benzene or carbon tetrachloride solution in the concentration range 10^{-6}–10^{-2} M is present largely as the dimer, chlorophyll$_2$. At concentrations $> 10^{-2}$ M, further aggregation of the dimer occurs in these solvents, and at 10^{-1} M the aggregation number measured by vapor phase osmometry is close to 4. In agreement with these observations, deconvolution of chlorophyll *a* spectra (Table II) in benzene or carbon tetrachloride over the concentration range 10^{-6}–10^{-2} M shows little variation and the deconvolution components are essentially identical. Between 10^{-2} and 10^{-1} M, however, a sharp decrease in the relative area of the 668-nm component relative to the 682-nm component is observed. At the higher concentrations, δ, the band half width of the 682-nm component also increases. Note that the effect of increasing concentration is reflected in a change in the relative areas of the 668- and 682-nm components, and not by change in the wavelengths at which the components are placed. Over the concentration range in which the chlorophyll *a* is present as dimer, as determined by independent physical measurements, the computer deconvolution is essentially invariant. When higher aggregates are formed in more concentrated solutions, it is only the relative areas of the bands that change, not their wavelengths. We wish to emphasize this point, as it is the most significant experimental finding in our work.

Deconvolution of chlorophyll oligomer spectra

In cycloaliphatic or aliphatic hydrocarbon solvents chlorophyll *a* has been shown to form oligomers by the equilibrium, $n(\text{chlorophyll}_2) \rightleftarrows (\text{chlorophyll}_2)_n$. In benzene or carbon tetrachloride, n is essentially 1 for chlorophyll *a* concentrations below 10^{-2} M. In hydrocarbon solvents, at high chlorophyll *a* concentrations, $n > 10$. Elevated temperatures and low chlorophyll *a* concentrations ($< 10^{-3}$ M) favor disaggregation to dimer, high chlorophyll *a* concentrations, and low temperature favor aggregation. The equilibrium is strongly solvent dependent. Soft, polarizable nonpolar solvents (benzene, carbon tetrachloride, 1,2-dichloroethane, xylene) displace the equilibrium to the left, aliphatic hydrocarbon solvents force the equilibrium to the right. Cyclohexane is intermediate in behavior.

Deconvolution data for cyclohexane solution of chlorophyll *a* are given in Table III. By extrapolation, we can speculate that the basic chlorophyll *a* species present in very dilute cyclohexane solutions is the dimer. Table III indicates that spectral characteristics of the dimer in dilute cyclohexane solutions are somewhat different from that of the dimer in benzene or carbon tetrachloride. The principal components (λ_3 and λ_4) are at 668 and 683 nm in CCl_4, but are at 664 and 678–679 nm in cyclohexane. It might be argued that this is only a solvent effect on the spectra, which may well be true to some extent, but the relative areas of the two components are significantly different in the two solvent systems, with the 679-nm component in the cyclohexane solutions present to a considerably greater extent than the corresponding component in carbon tetrachloride. We take these differences to indicate different populations of conformers in the two dimers. In addition, a marked change occurs in the relative areas of the 664- and 678-nm components in cyclohexane at higher chlorophyll *a* concentrations. In 10^{-1} M solution of chlorophyll *a* in carbon

TABLE III

GAUSSIAN COMPONENTS OF THE DECONVOLUTED RED ENVELOPE OF CHLOROPHYLL *a* IN AGGREGATING SOLVENTS

Concn (M)	λ_1 (nm)	δ_1 (nm)	% total area	λ_2 (nm)	δ_2 (nm)	% total area	λ_3 (nm)	δ_3 (nm)	% total area	λ_4 (nm)	δ_4 (nm)	% total area	λ_5 (nm)	δ_5 (nm)	% total area
Cyclohexane															
$1.43 \cdot 10^{-6}$	623	15	24	650	10	11	664.7	7.0	34	679.0	6.4	29	691.6	6.4	3
$1.4 \cdot 10^{-5}$	623	15	24	650	10	12	664.3	6.7	30	678.8	6.9	32	694.6	6.9	2
$2.72 \cdot 10^{-3}$	623	15	25	650	10	11	664.3	6.9	29	678.9	7.3	32	695.4	7.3	3
$2.2 \cdot 10^{-2}$	623	15	26	650	10	11	663.9	7.0	25	678.5	7.9	34	696.5	7.9	3
$1.2 \cdot 10^{-1}$	623	15	26	650	10	12	663.3	6.7	12	677.9	9.0	45	701	9.0	4
Dodecane															
$1.3 \cdot 10^{-6}$	624	19	29	650	10	6	663.2	7.1	33	678.0	6.8	30	695	6.8	2
$1.3 \cdot 10^{-5}$	624	19	30	650	10	6	663.2	7.0	32	677.9	6.8	30	695	6.8	2
$1.3 \cdot 10^{-4}$	624	19	30	650	10	6	663.2	7.1	31	677.9	6.9	31	695	6.9	2
	624	19	31	650	10	7	663.2	7.0	24	678.3	7.8	36	700	7.8	2
$1.2 \cdot 10^{-1}$	628	19	34	650	10	6	663.2	7.1	13	678.5	10.4	43	700	10.4	3
Hexane															
$1.09 \cdot 10^{-6}$	624	19	29	650	10	7	664.9	7.4	36	678.3	6.2	26	691.6	6.2	3
$1.3 \cdot 10^{-5}$	624	19	30	650	10	6	664.8	7.4	36	679.1	6.7	26	695.0	6.7	2
$1.3 \cdot 10^{-4}$	624	19	30	650	10	6	664.7	7.5	35	679.0	6.8	27	695.0	6.8	2
$2.46 \cdot 10^{-3}$	626	19	32.7	650	10	4.5	665.5	8.2	29.5	680.4	7.1	31	696.4	7.1	2.5
$3.8 \cdot 10^{-2}$	627	19	32	650	10	6	665.0	8.0	23	680.0	8.3	37	700	8.3	3
$6.0 \cdot 10^{-2}$	628	19	32	650	10	5	665.0	8.0	22	680.1	8.6	36	700	8.6	4
$9.6 \cdot 10^{-2}$	628	19	33	650	10	6	665.0	8.0	21	680.6	8.9	36	700	8.9	4
$1.2 \cdot 10^{-1}$	628	19	33	650	10	6	665.0	8.0	19	680.7	9.1	37	700	9.1	5

tetrachloride the 667 and 683 nm components are about equal in area (Table II), but in the corresponding cyclohexane solution, the 678-nm component is almost 4 times the size of the 663-nm component. This large change is entirely consistent with the point of view that there is a conformational change associated with change in the degree of aggregation as indicated by vapor phase osmometry molecular weight measurements; these measurements show 10^{-1} M chlorophyll *a* in cyclohexane to have an aggregation number of at least 10 as compared to a value in carbon tetrachloride at the same concentrations of less than 4.

Figs 1 and 2 show graphically deconvolutions for chlorophyll *a* solutions in hexane and dodecane as a function of concentration. Details of wavelength position,

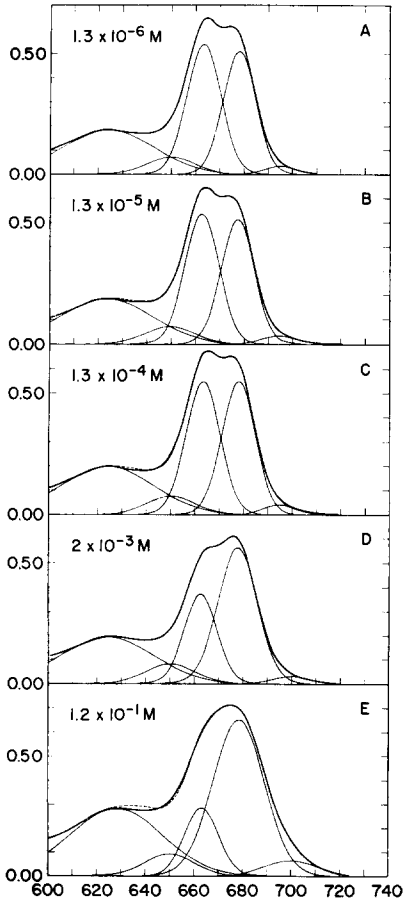

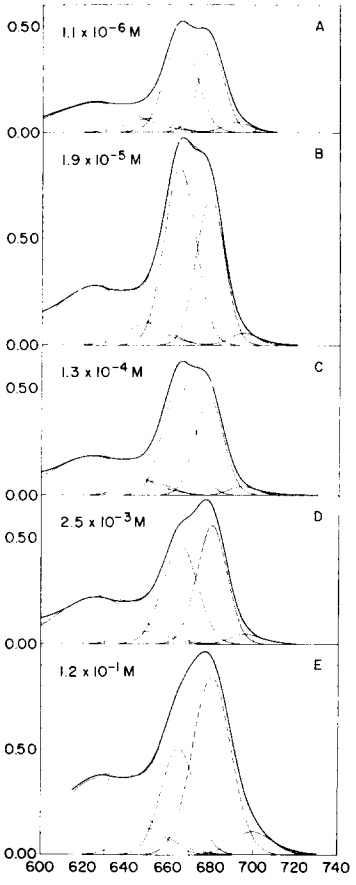

Fig. 1. Effect of concentration on the absorption spectrum of chlorophyll *a* in hexane. Abscissa = wavelength in nm; ordinate = absorbance. A, $1.3 \cdot 10^{-6}$ M solution; 10 cm pathlength cell; B, $1.3 \cdot 10^{-5}$ M solution; 1 cm pathlength cell; C, $1.3 \cdot 10^{-4}$ M solution; 1 mm pathlength cell; D, $2.0 \cdot 10^{-3}$ M solution; 0.05 mm pathlength cell; E, $1.2 \cdot 10^{-1}$ M solution between epoxied glass plates.

Fig. 2. Effect of concentration on the absorption spectrum of chlorophyll *a* in dodecane. Abscissa = wavelength in nm; ordinate = absorbance. A, $1.1 \cdot 10^{-6}$ M solution; 10 cm pathlength cell; B, $1.9 \cdot 10^{-5}$ M solution; 1 cm pathlength cell; C, $1.3 \cdot 10^{-4}$ M solution; 1 mm pathlength cell; D, $2.5 \cdot 10^{-3}$ M solution; 0.05 mm pathlength cell; E, $1.2 \cdot 10^{-1}$ M solution between epoxied glass plates.

peak half widths and relative areas are collected in Table III. Here, as in previous examples, an increase in concentration is reflected in large changes in the proportion of the 663-nm and the 678-nm components. In hexane and dodecane solutions, this change is already evident at concentrations between 10^{-4} and 10^{-3} M. The effect of chain length of the aliphatic hydrocarbon solvent is of interest. A comparison of Figs 1 and 2 shows that at all concentrations, solutions of chlorophyll *a* in dodecane have spectra with lower percentages of the approximate 680-nm component than do comparable hexane solution spectra. This effect is even more marked with longer chain hydrocarbons, i.e., *n*-hexadecane. Preliminary ultracentrifugation studies do not indicate that chlorophyll *a* is aggregated to a lesser extent in dodecane than in hexane. This is entirely consistent with our point of view that the approximate 680-nm component is related to the overlap of the π-orbitals of the nearest neighbor molecules and is indicative of the distribution of the conformer populations of the dimer or oligomer in a given solvent.

Degree of aggregation and the deconvoluted spectra

In a general way, there is clearly a relationship between conformer populations, aggregation and the relative area of λ_3 (668–669 nm) and λ_4 (678–679 nm). As solutions become sufficiently concentrated to displace the equilibrium in the direction of oligomer, the red Gaussian component, λ_4, increases in area at the expense of λ_3. In every case so far examined, a correlation exists between aggregate size as established by vapor phase osmometry and the relative areas of λ_3/λ_4, for a given solvent. That aggregation is, in fact, responsible for the changes in the spectra is further supported by experiments with chlorophyll *a*–pheophytin *a* mixtures. Chlorophyll *a* can function both as electron donor (magnesium) and donor (keto C=O), whereas pheophytin *a* can act only as donor. As shown by fluorescence spectrophotometry, chlorophyll *a* and pheophytin *a* do experience donor–acceptor interaction. Thus, in a 1 : 1 chlorophyll *a*–pheophytin *a* mixture, pheophytin *a* acts as a chain-breaker for chlorophyll *a* oligomer formation. The absorption spectrum of a 1 : 1 chlorophyll *a*–pheophytin *a* mixture does not change significantly between 10^{-4} and 10^{-1} M in cyclohexane. Thus, even though concentration changes, the extent of chlorophyll *a* aggregation does not change and there is no change in conformer populations.

The aggregate size, however, cannot be deduced from deconvolution data alone. A comparison of the relative areas of λ_3/λ_4 for solutions known to contain the same size chlorophyll aggregate (i.e., 10^{-4} M carbon tetrachloride and 10^{-4} M cyclohexane) as expected do not have quite the same deconvolution parameters. In all solvent systems, the changes observed with increasing concentration are qualitatively similar, but the quantitative aspects are different. Whether the differences are to be construed as solvent effects in the spectra or have some other basis requires consideration of the origin of the spectra and the physical significance of the deconvolution components.

Origin of the spectra

At this stage in the development of theory, it is still not possible to give a completely satisfactory molecular orbital description of the electronic transition spectra of chlorophyll *a*, its dimers and oligomers. The red band as seen in chlorophyll *a* monomer spectra must be considered to arise from electron π–π^* transition, whose

intensity and wavelength is related to the interaction of dihydropyrrole rings present in the macrocycle. Of most interest here are the factors involved in the genesis of the red shoulder. In agreement with earlier workers [56], we consider that the exciton theory of Hochstrasser and Kasha [57], Kasha [58], and McRae and Kasha [59] provides a suitable basis for the origin of the red shoulder. Exciton theory indicates that the red shift is a result of cooperative interaction between two or more chlorophyll *a* molecules. An examination of laboratory data, however, indicates all interactions of the type, chlorophyll · L_1 or chlorophyll · L_2, in which chlorophyll *a* molecules are substantially isolated from each other are short wavelength forms in which the red maxima occurs between about 660 and 665 nm. (Chlorophyll *a* in neat pyridine absorbs at 672 nm. Seely [8] has shown, and we have confirmed, however, that chlorophyll · pyridine in hydrocarbon solvents is blue-shifted (662 nm) and that the absorption maximum in neat pyridine is probably the result of a solvent shift.)

As described in Introduction, chlorophyll *a* molecules can be brought into juxtaposition either by (a) keto C=O · · · Mg (endogamous) interactions, or by (b) (exogamous) interactions with bifunctional electron–donor ligands. NMR investigations show that the extent of the overlap between the chlorophyll *a* rings of the dimer must be small, and, indeed the rings cannot be forced into a parallel orientation in solution at room temperature as long as keto C=O · · · Mg interactions are the presumed force for cohesion. Bifunctional ligands (dioxane, pyrazine, etc.) act as electron donor to two magnesium atoms simultaneously. They can thus cross-link chlorophyll *a* monomers and/or dimers to form large fairly well-structured aggregates. The extent of ring overlap in these chlorophyll *a* adducts with bifunctional ligands appears to be greater than is the case in dimers or oligomers. Continued aggregation of chlorophyll *a* dimers to oligomers results in intensity changes in the spectrum and not in shifts in the position of the maxima. From this point of view, an attempt can be made to assess the physical significance of the Gaussian components into which the red envelope of chlorophyll *a* can be deconvoluted.

Physical significance of the Gaussian components

We consider first the structure of chlorophyll *a* dimer and how it may be related to its electronic transition spectra. It appears plausible to consider the red shoulder as a consequence of exciton splitting arising from interactions between dihydroporphyrin rings, and the geometry of the dimer will determine the electronic transition spectra. NMR studies indicate the dihydroporphyrin rings in chlorophyll *a* dimer in chloroform solution are oriented at a small angle to each other; ring current considerations suggest this angle to be about 30° in this solvent. Houssier and Sauer [60], from circular dichroism measurements in carbon tetrachloride, deduce an angle of 45° between the ring planes. The different conformers of chlorophyll *a* dimer will have different ring overlap and therefore different spectra. On the NMR time scale, only an average dimer structure is seen, but electron transitions are very fast relative to the motions of the rings in the dimer, and the spectra must therefore reflect populations of the different possible dimer conformations. Thus, in a perpendicular dimer ($\perp\!\!\perp$) structure little perturbation of the transition dipoles of either molecule occurs. In a parallel structure* ($=$) there is more interaction and a dimer with such orientation

* These schematic diagrams should not be interpreted too literally. They are meant to illustrate limiting forms of the dimer.

would be expected to have a quite different electronic transition spectrum. A small decrease in the angle from 90° should produce a blue-shifted component relative to the monomer absorption; we can speculate that this orientation could contribute to the "hidden" 650-nm component. Low temperature studies, to be discussed in detail elsewhere, also support the conformational interpretation of the dimer and oligomer absorption spectra. In chlorophyll *a*–*n*-octane solutions at −1 °C all of the 678-nm band is converted into a 695-nm band, while the component near 665 nm is not shifted appreciably. The red Gaussian band shift can be interpreted to result from a change in the average orientation in the dimer, which is expected to be very sensitive to temperature and to the solvent. In fact, both NMR and electronic transition spectra are highly temperature dependent. NMR also confirms that there are real differences between the structure of the dimer in various nonpolar solvents. The NMR spectra are very much better resolved and less subject to chlorophyll *a* ring current effects in benzene, 1,2-dichloroethane, and chloroform than in carbon tetrachloride. A solvent dependence of dimer structure can account for the small but real difference that can be detected in the deconvoluted spectra.

Consideration of the Gaussian components in these terms affords an explanation of the inability to correlate precisely the area of the Gaussian components with the degree of aggregation, because the degree of aggregation also influences the geometry of the aggregate. The average geometry of the chlorophyll *a* aggregates represents the weighed average of various conformer populations. From the study of structural changes of chlorophyll *a* dimers in carbon tetrachloride and benzene in the presence of shift reagents we have substantiated both by ^{1}H NMR and electronic transition spectroscopy that the approximate 680-nm component is related to the degree of macrocycle overlap in the chlorophyll *a* dimers [61].

It is well known that the approximate 665-nm (monomer) band is intrinsic to the macromolecular system, and that the approximate 680-nm band can be properly called an interaction band. The relative importance of these two bands in the chlorophyll *a* dimer or oligomer spectra is related to the prevalent geometry, that is conformer population, since the band intensity is a consequence of the geometric relationship of transition dipole moments. The interaction of the transition moments is known to be approximately dependent on the separation between the macrocycle by a factor proportional to $1/r^3$, where r is the distance of separation. Thus, it is not surprising that the nearest neighbor interactions are dominant in determing the general appearance of the electronic transition spectra. One of the general results of the molecular exciton treatment is that the number of allowed levels within an exciton band is equal to the number of molecules per unit cell in the lattice [57]. Thus, if the (chlorophyll$_2$) dimer unit is a building block of the more aggregated forms of chlorophyll *a*, it is not surprising that the dimer splitting is a most dominant one. The interaction of the transition dipole moments in the dimer with next-to-nearest neighbor macrocycles as in a chlorophyll *a* trimer would be expected to result in other interaction bands. These higher order interactions, however, are either too small or cannot be separated from the larger dimer contributions. It seems reasonable to suppose that these higher order interactions contribute to the manifold of states, resulting from the largest interaction, only by splitting them slightly and by influencing their transition probabilities. This would be manifest by an increase in the area of the red component and a broadening of its band width. The schematic drawing of a

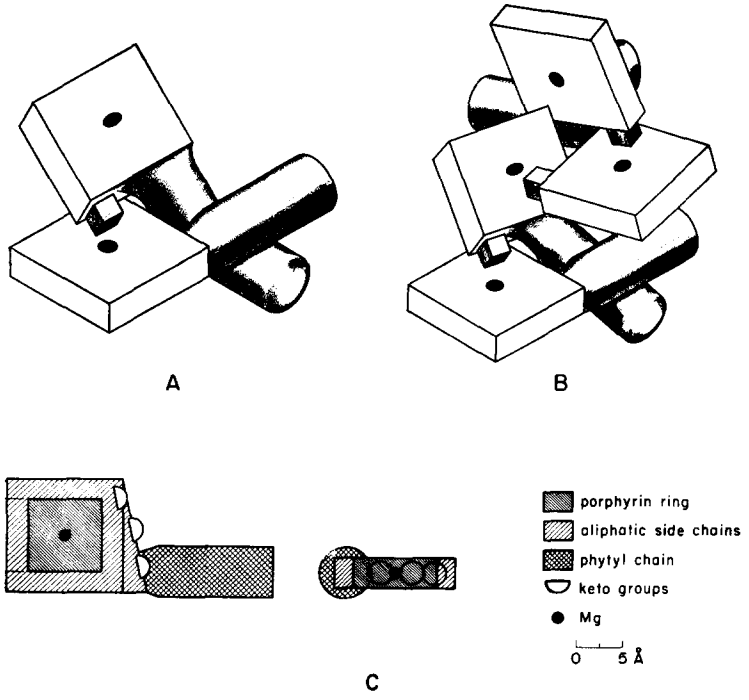

Fig. 3. Aggregate structures of chlorophyll *a* dimers (A) and oligomers (B) as taken from Courtould models.

generalized model of chlorophyll *a* dimer and oligomer is shown in Fig. 3. A precise and detailed geometrical picture of the chlorophyll *a* dimers and oligomers cannot be advanced at this time. From our data we see that as a consequence of aggregation there must be tilting and rotation of the macrocycle planes of the chlorophyll *a* molecules in more highly aggregated species. This is reflected in the increase in the π-overlap of the two molecules. That is, in a dynamic equilibrium present in the dimer and oligomer solutions there is an increase in population of conformers that have more ring overlap, thus giving rise to an increase in the red component in the electronic transition spectra.

It is important to emphasize that by "conformer population" we do not imply a strict one-to-one correspondence between the intensity of the bands obtained by the deconvolution of the envelopes of the visible spectra, and the population of the various conformation of chlorophyll *a* dimers and oligomers. The M.O. description of the chlorophyll *a* dimer and oligomer by "transition dipole" and "transition monopole" approximations is in agreement with our interpretation of the general features of the chlorophyll *a* electronic transition spectra. However, these M.O. approaches further emphasize the complexity and the need for improving our simplified point of view in these matters [62].

Deconvolution of in vivo spectra

While the computer deconvolution of the red envelope of the chlorophyll *a*

spectrum must still be regarded essentially as an heuristic approach, its serves to define in a more precise way than previously possible the spectral consequences of chlorophyll–chlorophyll self-aggregation. We have, therefore, applied these same procedures to the in vivo chlorophyll *a* spectra. As is well-known, visible absorption spectra of intact photosynthetic organisms, sonicates, or active center preparations collected at room temperature are essentially without structure, and unique computer deconvolutions cannot be obtained on such systems per se [45]. Consequently, most computer deconvolutions hitherto reported on in vivo systems have been carried out on spectra recorded at cryogenic temperatures. We regard such data with a certain unease, as there is good reason to suppose that strong cooling serves not only to sharpen the spectra, but also results in changes in the conformation of the chlorophyll *a* species present. Consequently, we question the relationship of the room temperature chlorophyll *a* species and the low temperature species. The procedures we describe here, however, make possible an examination of the in vivo spectra recorded at room temperature.

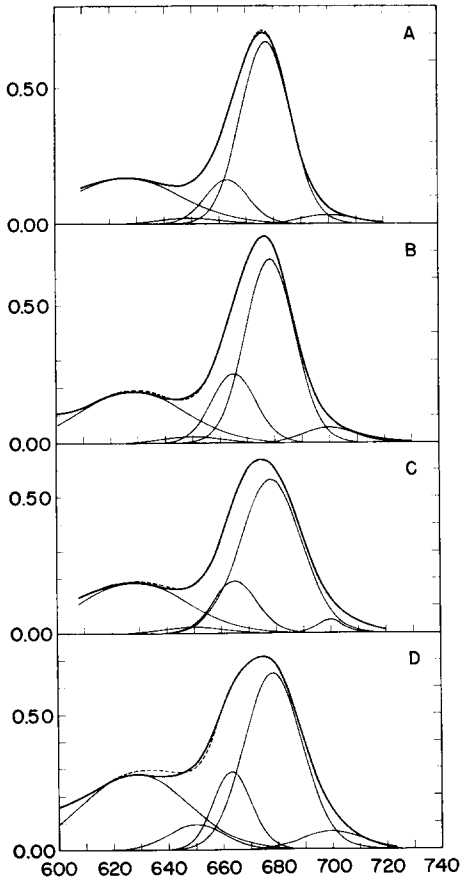

Fig. 4. Comparison of deconvolution of chlorophyll *a* red envelope in vivo and of chlorophyll *a* oligomers in *n*-hexane solution. Abscissa = wavelength in nm; *Tribonema aequale* sonicate; (B) *S. lividus* HP700; (C) *A. variabilis* HP700; (D) chlorophyll *a* in *n*-hexane; concn = $1.2 \cdot 10^{-1}$ M.

We have recorded the visible absorption spectra at room temperature of intact and sonicated *Tribonema aequale*, a green alga containing only chlorophyll *a* and no other chlorophyll or phycobilin auxilliary pigments, and of active center preparations prepared by methods of Vernon et al. [63] from the blue-green algae *Anabaena variabilis* and *Synechococcus lividus*, where the auxilliary phycobilins are removed during preparation. In all of these spectra, the red envelope can be fitted very well (Fig. 4) with precisely the same Gaussian components as are required for the deconvolution of solutions of chlorophyll *a* in hexane over the concentration range 10^{-5}–10^{-1} M. The deconvoluted spectra of plant material resemble most closely those of concentrated ($> 10^{-1}$ M) solutions of chlorophyll *a* in hexane or other aliphatic hydrocarbon solvents. As can be seen from Fig. 4, the similarity between the deconvoluted spectra of plant material and of chlorophyll *a* oligomers in hexane is striking. We consider this as good presumptive evidence for a structural similarity, or even identity, between chlorophyll *a* oligomer, $(\text{chlorophyll}_2)_n$, and antenna chlorophyll *a* in green plants.

The identification of antenna chlorophyll *a* as chlorophyll *a* oligomers, $(\text{chlorophyll}_2)_n$, of course implies that antenna chlorophyll *a* in the plant exists in a strongly hydrophobic environment similar to that of an aliphatic hydrocarbon solvent to which access of water is severely limited, as the introduction of water in such an environment would lead to the formation of strongly red-shifted chlorophyll *a*-water adducts. In fact, Lippincott and co-workers [64, 65] observed a conversion by treatment with organic, water-soluble solvents of antenna chlorophyll *a* in tobacco chloroplasts to a chlorophyll *a* species with a visible absorption spectrum and electron spin resonance properties identical to those of the chlorophyll *a*–water adduct $(\text{chlorophyll} \cdot H_2O)_n$ in vitro [4]. Chlorophyll *a* oligomer is stable only in highly hydrophobic environments, and thus we can take the observations of Lippincott et al. as additional confirmation of the requirement that antenna chlorophyll *a* occur in the plant in an environment remarkably similar to aliphatic hydrocarbons in polarity. The suggestion advanced by Fisher et al. [66] and Strouse [67] that antenna chlorophyll *a* in the plant is the chlorophyll *a*–water adduct described by Katz et al. [2] is clearly incompatible with the visible absorption spectra of chlorophyll *a*–water adducts, which are all much more strongly red-shifted (> 730 nm) than is either antenna chlorophyll *a* in the plant or chlorophyll *a* oligomer. Chlorophyll *a*–water adducts do, however, provide a model for photo-active chlorophyll *a* in plants, and this combined with the proposal advanced here that antenna chlorophyll in green plants lacking chlorophyll *b*★ can be identified with chlorophyll *a* oligomers provides the basis for a new hypothesis for the nature of the photosynthetic unit in vivo [68].

REFERENCES

1 Clayton, R. K. (1973) Annu. Rev. Biophys. Bioeng. 2, 131–156
2 Katz, J. J., Ballschmiter, K., Garcia-Morin, M., Strain, H. H. and Uphaus, R. A. (1968) Proc. Natl. Acad. Sci. U.S. 60, 100–107

★ We can speculate that the incorporation of chlorophyll *b* into a chlorophyll *a* antenna will not radically affect the spectral consequences of chlorophyll *a* aggregation, but this point is under investigation.

3 Garcia-Morin, M., Uphaus, R. A., Norris, J. A. and Katz, J. J. (1969) J. Phys. Chem. 73, 1066–1070
4 Norris, J. R., Uphaus, R. A., Crespi, H. L. and Katz, J. J. (1971) Proc. Natl. Acad. Sci. U.S. 68, 625–628
5 Norris, J. R., Uphaus, R. A. and Katz, J. J. (1972) Biochim. Biophys. Acta 275, 161–168
6 Rabinowitch, E. (1951) in Photosynthesis II, pp. 603–649, Wiley–Interscience, New York
7 Seely, G. R. and Jensen, R. G. (1965) Spectrochim. Acta 21, 1835–1845
8 Seely, G. R. (1965) Spectrochim. Acta 21, 1847–1856
9 Sauer, K., Smith, J. R. L. and Schultz, A. J. (1966) J. Am. Chem. Soc. 88, 2681–2688
10 Amster, R. L. (1969) Photochem. Photobiol. 9, 331–338
11 Amster, R. L. and Porter, G. (1966) Proc. Royal Soc. 296, 38–44
12 Livingston, R. (1960) Q. Rev. 14, 174–199
13 Livingston, R., Watson, W. F. and McArdle, J. (1949) J. Am. Chem. Soc. 71, 1542–1550
14 Freed, S. (1957) Science 125, 1248–1249
15 Fernandez, J. and Becker, R. S. (1959) J. Chem. Phys. 31, 467–472
16 Lavorel, J. (1957) J. Phys. Chem. 61, 1600–1605
17 Rabinowitch, E. (1945) in Photosynthesis I, p. 412, Wiley–Interscience, New York
18 Goedheer, J. C. (1966) in The Chlorophylls (Seely, G. R. and Vernon, L. P., eds) pp. 147–184, Academic Press, New York
19 Sherman, G. and Fujimori, E. (1969) Arch. Biochem. Biophys. 130, 624–628
20 Ballschmiter, K. and Katz, J. J. (1968) Nature 220, 1231–1233
21 Ballschmiter, K. and Katz, J. J. (1972) Biochim. Biophys. Acta 256, 307–327
22 Katz, J. J., Closs, G. L., Pennington, F. C., Thomas, M. R. and Strain, H. H. (1963) J. Am. Chem. Soc. 85, 3801–3809
23 Anderson, A. F. H. and Calvin, M. (1964) Arch. Biochem. Biophys. 107, 251–259
24 Boucher, L. J., Strain, H. H. and Katz, J. J. (1966) J. Am. Chem. Soc. 88, 1341–1348
25 Boucher, L. J. and Katz, J. J. (1967) J. Am. Chem. Soc. 89, 1340–1345
26 Boucher, L. J. and Katz, J. J. (1967) J. Am. Chem. Soc. 89, 4703–4708
27 Henry, M. and Leicknam, J.-P. (1970) Colloq. Int. C.N.R.S. 191, 317–333
28 Closs, G. L., Katz, J. J., Pennington, F. C., Thomas, M. R. and Strain, H. H. (1963) J. Am. Chem. Soc. 85, 3809–3821
29 Katz, J. J., Dougherty, R. C. and Boucher, L. J. (1966) in The Chlorophylls (Vernon, L. P. and Seely, G. R., eds), pp. 185–251, Academic Press, New York
30 Katz, J. J., Strain, H. H., Leussing, D. L. and Dougherty, R. C. (1968) J. Am. Chem. Soc. 90, 784–791
31 Katz, J. J. and Crespi, H. L. (1972) Pure Appl. Chem. 32, 221–250
32 Katz, J. J. (1968) Dev. Appl. Spectr. 6, 201–218
33 Katz, J. J., Janson, T. R., Kostka, A. G., Uphaus, R. A. and Closs, G. L. (1972) J. Am. Chem. Soc. 94, 2883–2885
34 Ballschmiter, K., Truesdell, K. and Katz, J. J. (1969) Biochim. Biophys. Acta 184, 604–613
35 Katz, J. J. (1973) in Inorganic Biochemistry (Eichhorn, G. L., ed.), Vol. II, pp. 1022–1066, Elsevier, Amsterdam
36 Ballschmiter, K. and Katz, J. J. (1969) J. Am. Chem. Soc. 91, 2661–2677
37 Smith, J. H. C. and French, C. S. (1963) Annu. Rev. Plant Physiol. 14, 181–224
38 Brown, J. S. (1963) Photochem. Photobiol. 2, 159–173
39 Brown, J. S. (1972) Annu. Plant Physiol. 23, 73–86
40 French, C. S. (1971) Proc. Natl. Acad. Sci. U.S. 68, 2893–2897
41 French, C. S. and Prager, L. K. (1969) in Progr. Photosyn. Res. 2, 555–564
42 French, C. S., Michel-Wolwertz, M. R., Michel, J. M., Brown, J. S. and Prager, L. K. (1969) in Porphyrins and Related Compounds (Goodwin, T. W., ed.), Vol. 28, pp. 147–162, The Biochemical Society Symposium, Academic Press, New York
43 Wiessner, W. and French, C. S. (1970) Planta 94, 78–90
44 French, C. S., Brown, J. S., Wiessner, W. and Lawrence, M. C. (1971) Carnegie Inst. Wash. Yearb. 69, 662–670
45 French, C. S., Brown, J. S. and Lawrence, M. C. (1971) Carnegie Inst. Wash. Yearb. 60, 487–495
46 Cederstrand, C. N., Rabinowitz, E. and Govindjee (1966) Biochim. Biophys. Acta 126, 1–12
47 Gulyaev, V. A. and Litvin, F. F. (1967) Biofizika (Engl. Transl.) 12, 970–980

48 Gulyaev, V. A. and Litvin, F. F. (1970) Biofizika (Engl. Transl.) 15, 701–712
49 Strain, H. H. and Svec, W. A. (1966) in The Chlorophylls (Vernon, L. P. and Seely, G. R., eds), pp. 21–66, Academic Press, New York
50 Ballschmiter, K., Cotton, T. M., Strain, H. H. and Katz, J. J. (1969) Biochim. Biophys. Acta 180, 347–359
51 Chamot, C. (1967) in Integration of Gaussian Spectral Lines, C-151, Argonne Program Library, Argonne National Laboratory, Argonne
52 Davidon, W. C. (1966) in Variable Metric Method for Minimization, ANL-5990 (Rev. 2), Argonne National Laboratory, Argonne
53 Van Vleck, J. H. (1956) Nvovo Cimento, Suppl. to Vol. VI, 993–1014
54 Katz, J. J. (1973) Naturwissenschaften 60, 32–39
55 McCartin, P. J. (1963) J. Phys. Chem. 67, 513–515
56 Brody, S. S. and Brody, M. (1961) Biochim. Biophys. Acta 54, 495–505
57 Hochstrasser, R. M. and Kasha, M. (1964) Photochem. Photobiol. 3, 317–331
58 Kasha, M. (1959) Rev. Mod. Phys. 31, 162–169
59 McRae, E. G. and Kasha, M. (1958) J. Chem. Phys. 28, 721–722
60 Houssier, C. and Sauer, K. (1970) J. Am. Chem. Soc. 2, 779–791
61 Trifunac, A. D. and Katz, J. J. (1974) J. Am. Chem. Soc., 96, 5233–5240
62 Chang, Jane C. E. (1972) Ph. D. Thesis, University of Rochester, New York
63 Vernon, L. P., Yamamoto, H. Y. and Ogawa, T. (1969) Proc. Natl. Acad. Sci. U.S. 63, 911–917
64 Lippincott, J. A., Aghion, J., Porcile, E. and Bertsch, W. F. (1962) Arch. Biochem. Biophys. 98, 17–27
65 Lippincott, J. A. and Lippincott, B. B. (1964) Arch. Biochem. Biophys. 105, 359–366
66 Fischer, M. S., Templeton, D. H., Zalkin, A. and Calvin, M. (1972) J. Am. Chem. Soc. 94, 3613–3619
67 Strouse, C. E. (1974) Proc. Natl. Acad. Sci. U.S. 71, 325–328
68 Katz, J. J. and Norris, J. R. (1973) in Current Topics in Bioenergetics (Sanadi, D. R. and Packer, L., eds), Vol. 5, pp. 41–75, Academic Press, New York